



# Influence of water content on structural and electrochromic properties of TiO<sub>2</sub> nanotube prepared by anodization

Chantana AIEMPANAKIT<sup>1</sup>, Pathomporn JUNBANG<sup>2</sup>, Watchara SUPHAP<sup>3</sup>, and Kamon AIEMPANAKIT<sup>3,\*</sup>

<sup>1</sup> Division of Physics, Faculty of Science and Technology, Rajamangala University of Technology Thanyaburi, Pathumthani, 12110, Thailand

<sup>2</sup> Department of Physics, Faculty of Medicine, Bangkokthonburi University, Thawi Watthana, Bangkok, 10170, Thailand

<sup>3</sup> Department of Physics, Faculty of Science and Technology, Thammasat University, Pathumthani, 12121, Thailand

\*Corresponding author e-mail: akamon@staff.tu.ac.th

## Received date:

13 March 2023

## Revised date

28 June 2023

## Accepted date:

29 June 2023

## Keywords:

TNTs;  
Anodization;  
Annealing;  
Energy gap;  
Electrochromic

## Abstract

TiO<sub>2</sub> nanotubes (TNTs) and bamboo-type TNTs structure films were synthesized via anodization from sputtered titanium (Ti) films on indium tin oxide (ITO) glass. Herein, the anodization process was adjusted electrolyte with different amounts of deionized water and ethylene glycol. The optical and structural properties of all films before and after annealing were investigated, which affected electrochromic application. The increasing deionized water content in electrolytes resulted in an increase in the average diameter and a decrease in the average length of TNTs. Furthermore, the bamboo-type TNTs structure was produced at the deionized water volume condition of 3 vol%. The crystallite size of annealed TNTs (a-TNTs) was calculated from the Scherrer equation, which was enhanced when increasing deionized water. TNTs conditions before annealing showed that the amorphous structure and high energy band gap ( $E_g$ ) exhibited more electrochromic phenomena than the crystal structure. Due to the disordered arrangement of structures, it was easy to insert ions in TNTs. The bamboo-like structure with separate tubes increased the surface area of the reaction, thus exhibiting the best electrochromic properties with  $\Delta T$  equal to 12.58%.

## 1. Introduction

Titanium dioxide (TiO<sub>2</sub>) films are an excellent candidate material and use preparation as nanostructures to increase the efficiency of sensors [1,2], solar energy [3], photocatalytic activity [4,5], and electrochromic [6,7] applications. The advantages of nanostructures such as nanorods [8], nanofibers [9,10], nanowires [11], and nanotubes [12,13] are used to increase the active surface area in applications. Nanotube structures have attracted a lot of attention due to their distinctive features such as orderly arrangement and easy increase in tube length and diameter. In most cases, the preparation of nanotubes is commonly done by anodization technique which studied the influence of various variables including the type and concentration of the electrolyte solution and difference voltage [14-19]. These parameters change the morphological structure of the tube in relation to its optical properties, crystal structure, electrical properties, and surface area.

Yang *et al.* [11] investigated and compared the effects of H<sub>2</sub>O<sub>2</sub> and H<sub>2</sub>O content on the anodizing current and morphology of TNTs and obtained ginseng-like nanotubes. Sergiu *et al.* [18] have developed TNTs a structure that can be built into bamboo-like and nanolace sheets by an anodization process carried out under specific alternating-voltage conditions. Kim *et al.* [20] developed a bamboo-like TNTs structure to increase the efficiency of dye-sensitized solar cells.

In addition, Regonini *et al.* [13] reported that controlling the amorphous structure to the crystal phase transition of anatase to rutile

of TNTs was systematically heat treated in the temperature range of 200°C to 600°C. Siuzdak *et al.* [21] improved crystallization of TNTs within an area limited by laser treatment. Ghicov *et al.* [22] exhibited a high storage capacity for H<sup>+</sup> for the TNTs for electrochromic properties, while Yao *et al.* [7] used MoO<sub>3</sub> deposited on TNTs for increased intercalation probability and also provided direct pathways for charge carrier transfer. The development of TNTs structures was under the condition of the variable factors of the film preparation process. From these reviews, it can be seen that the changes in the structure of TNTs as well as their morphology and crystallinity are of great interest and have implications for their applications. Among the applications of TNTs films, this unique structure greatly increases the reaction surface area and is expected to be suitable for use in electrochromic properties. Since TiO<sub>2</sub> is a material that exhibits electrochromic properties [10,11,21,22]. Moreover, TiO<sub>2</sub> is used as a good anti-corrosion film [23]. Generally, electrochromic properties are used in the development of smart windows to reduce the problem of thermal energy from light, especially in the visible and infrared ranges. Popular materials are WO<sub>3</sub> [24-27] and NiO [28-30] films, which have good electrochromic properties. But there are easily deteriorated during use. Therefore, the development of TNTs structures was of great interest to their electrochromic applications as an additional efficient alternative.

In this work, the TNTs films preparation from the anodization technique altered the morphological structure of length, diameter,

and morphology. Moreover, the effects of annealing TNTs were investigated on their optical properties, crystal structure, and electrochromic. We deduced that annealing enhanced the crystal structure of TNTs while decreasing  $E_g$  and electrochromic properties. The bamboo-like structure of the TNTs films exerted a significant effect on enhancing electrochromic properties.

## 2. Experimental

### 2.1 TNTs synthesis

TNTs were anodized from sputtered Ti films on cleaned ITO glass substrates (2.50 cm × 3.00 cm). A Ti disc with 99.995% purity was used as the target (2 in. diameter and 0.25 in. thick, Kurt J. Lesker). The distance between the target and substrate was 8.0 cm. The sputtering chamber was pumped down with a rotary pump and diffusion pump to a base pressure of  $5 \times 10^{-5}$  mbar. Argon gas (99.999% pure) at a flow rate of 15 sccm (standard cubic centimeters per minute) was used for gas sputtering at a working pressure of  $2 \times 10^{-2}$  mbar. The sputtering power of 200 W was used to provide the Ti crystal structure [12]. The thickness of the Ti films was found to be approximately 835 nm. The glass/ITO/Ti films were anodized by using Ti film as the anode and lead as the cathode (4.00 cm apart) at a constant voltage of 30 V for 2 h under an electrolyte consisting of ethylene glycol (97 vol% to 99 vol%), deionized water (1 vol% to 3 vol%, henceforth denoted for TNTs1-TNTs3), and  $\text{NH}_4\text{F}$  (0.6 wt%). After anodization, the TNTs films were rinsed in deionized water for 15 s to remove any debris covering the top of the nanotubes. After that, the TNTs films were annealed (a-TNTs) in the air at 450°C for 1 h.

### 2.2 Characterization

The top view and cross-sectional morphologies of annealed TNTs films were examined using field emission scanning electron microscopy (FE-SEM, Tescan/Mira3, Czech Republic). The crystal structures of annealed TNTs films were determined by X-ray diffraction (XRD, Bruker, D2 Phaser) in the  $2\theta$  range of  $20^\circ$  to  $80^\circ$  using  $\text{CuK}\alpha$  radiation ( $\lambda=1.5406 \text{ \AA}$ ), the operating voltage of 30 kV and current of 10 mA.

The optical properties of TNTs and a-TNTs were examined with ultraviolet-visible spectroscopy (G10S UV-Vis, Thermo Scientific) in wavelengths between 300 nm and 1000 nm. The electrochromic properties of TNTs and a-TNTs films were tested under a 1.0 M KOH

solution by applying voltages of -0.8 V to +0.8 V at the colored and bleached states, respectively.

## 3. Results and discussion

Figure 1(a) shows a top view and cross-sectional FE-SEM image of sputtered Ti films with a thickness of 833 nm. The Ti films exhibited a large columnar-grained structure, which was achieved by high-sputtering atom energy. The sputtering power of 200 W is a high value for a 2-in. diameter target and the controlling plasma beam by the unbalanced magnetron is directed to the ITO substrate for self-heating. Generally, the sputtering of Ti film is preferred to heating the substrate to induce the formation of a crystal structure [14]. In this work, the results exhibited the crystal structure of Ti film, as shown in Figure 1(b), without external heating. This demonstrated an orderly and dense formation suitable for further anodization [12,31].

The Ti film restructured to TNTs by the anodization process [12] is shown in Figure 2. The difference in electrolyte solution between reduced ethylene glycol and increased deionized water resulted in very different tubular structures. This is because deionized water increases ions in the process and reduces the viscosity of the electrolyte solution. The effect of increasing the deionized water content has been reported to increase the TNTs diameter [15-17]. The results showed good concordance, as shown in Figure 3. In addition, the TNTs were separated from each other with deionized water of 3 (TNTs3). The TNTs3 showed a bridge of connected nanotubes. This resulted from the effect of the partial dissolution of the adjacent oxide ring and gave the nanotubes a bamboo-like structure. It also depends on some electrolyte constituents to form such a structure [18,20]. Herein, this resulted in a greater surface area, inside and outside the TNT, compared to other conditions (TNTs1 and TNTs2) that only have an internal surface area.

The as-prepared TNTs films were amorphous (not shown) and transformed into a crystal structure after annealing, as shown in Figure 4. The crystal structure of TNTs exhibited XRD diffraction peaks of  $2\theta$  at  $25.30^\circ$ ,  $37.87^\circ$ ,  $48.03^\circ$ , and  $53.98^\circ$  of a-TNTs1,  $25.28^\circ$ ,  $37.93^\circ$ ,  $48.37^\circ$ , and  $53.88^\circ$  of a-TNTs2, and  $25.28^\circ$ ,  $37.80^\circ$ ,  $48.05^\circ$ , and  $53.89^\circ$  of a-TNTs3 corresponded to the crystal planes of (101), (004), (200), and (105), respectively. The resulting crystal structure corresponded well with the anatase phase of  $\text{TiO}_2$  (PDF 03-065-5714). The a-TNT2 exhibited the highest intensity of the XRD peak, while the XRD intensity of aTNT3 was similar to that of aTNT1.

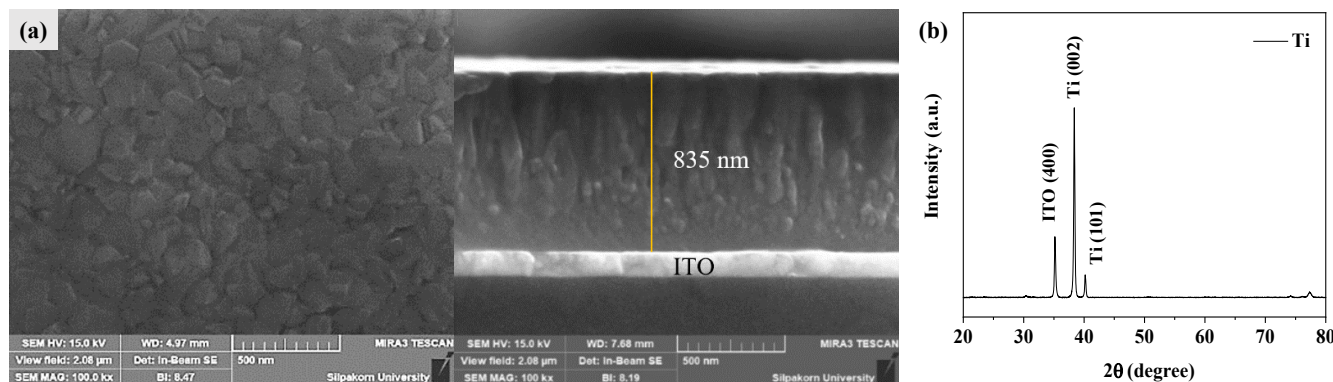


**Figure 1.** (a) FE-SEM images top view and cross-section view and (b) XRD pattern of sputtered Ti film.

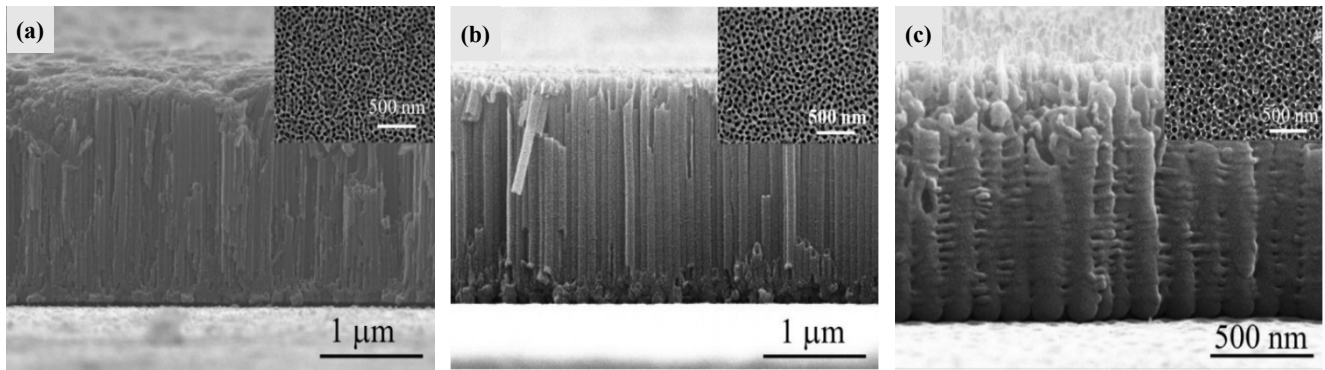


Figure 2. Cross sectional and top view FE-SEM images of (a) TNTs1, (b) TNTs2, and (c) TNTs3.

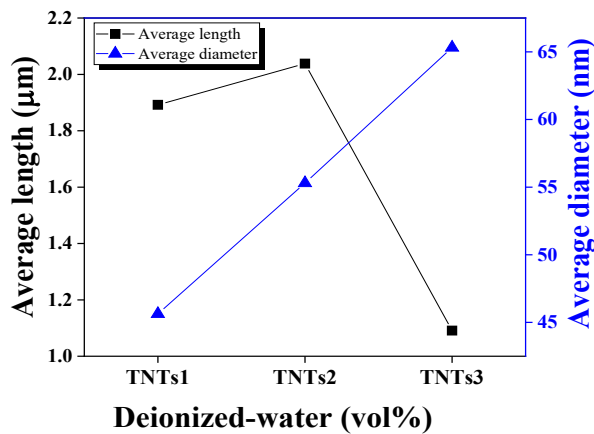


Figure 3. Average length and average diameter of TNTs.

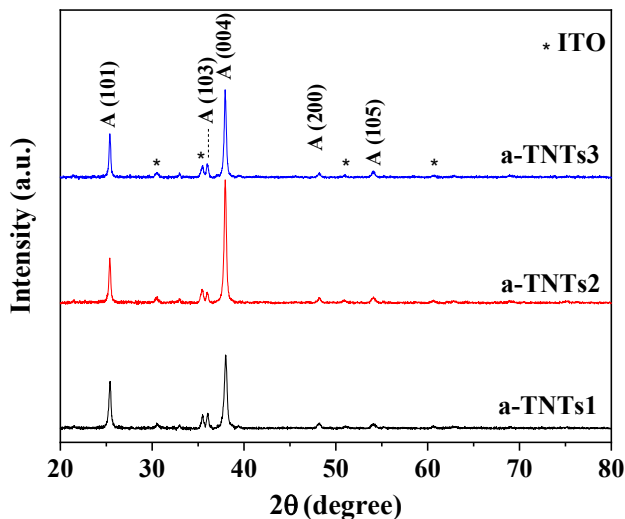


Figure 4. XRD peaks of a-TNTs.

Although all 3 conditional TNTs are annealed in the same condition, different morphological characteristics affect crystallinity. Generally, the tendency of higher film thickness enhances the intensity of an X-ray diffraction peak (as a-TNTs2) but lowers the thickness of a-TNTs3 appeared to intensity of XRD peaks, similar to TNTs1. Therefore, the larger diameter morphological structure and bamboo-like structure of a-TNT3 simplify the arrangement of the crystal structure for the reason that the surface area is high during annealing.

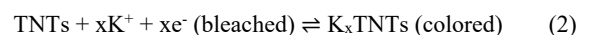
These results are appropriately consistent and acceptable for the formation of oxides to crystal structures with highly exposed surface area by annealing [8]. The crystallite size of the a-TNTs films was calculated from the Debye-Scherrer Equation (1). The a-TNTs1-3 exhibited average crystallite size at the (004) plane, which was 24.34, 29.53, and 30.61 nm, respectively, while crystallite size at the (101) plane was 26.68, 32.87, and 34.32 nm, respectively. The results showed that increasing the deionized water content enlarged the diameter of TNTs and increased the formation of crystallite size.

$$D = (k\lambda/\beta\cos\theta) \quad (1)$$

where  $D$  is the crystallite size,  $k$  is known as the Scherrer's constant,  $\lambda$  is the X-ray wavelength (1.5406 Å), and  $\beta$  is the full width at half maximum (FWHM) of the diffraction peak.

The optical properties are important for applications because TiO<sub>2</sub> films have high transparency and a large energy band gap [3-6]. For a nanotubular structure, the surface roughness and high length affected the optical scattering and absorption enhancement. In addition, TNTs annealing directly affects the optical properties. Figure 5 shows the Tauc plot for band gap determination [8] of TNTs before and after annealing. The energy band gap ( $E_g$ ) is obtained from the x-intercept by extrapolating the linear part between  $h\nu$  on the x-axis versus  $(\alpha h\nu)^{1/2}$  on the y-axis. As a result, the  $E_g$  decreased after annealing, which corresponded with the result of the crystal structure arrangement. Won *et al.* [32] studied the annealing effects of TiO<sub>2</sub> films on structural and optical properties. The results were consistent with lower transmittance, higher crystalline size, and lower  $E_g$  after annealing. One reason for the orderly arrangement of atoms in the crystal structure is that the energy gap approaches the value of the anatase phase (3.23 eV to 3.59 eV) [8,33]. Therefore, the larger diameter of a-TNTs affects the larger crystalline size and decreases the  $E_g$ .

TNTs films were tested for electrochromic properties under KOH electrolytes with an applied voltage of -0.8 V for the coloration stage and an applied voltage of +0.8 V for the bleached state. The general reaction of TNTs for the electrochromic properties is shown in Equation (2):



where  $x$  is the insertion coefficient of electrochromic activity, and  $\text{K}^+$  is potassium ions.

The colored state will be more or less depending on many factors, including defects in the structure, active surface area, the ability to diffuse ions, etc. [24-26,34]. The transmittance spectra of all TNTs and a-TNTs for colored and bleached states were investigated, as in Figure 6. The results showed that the transmittance decreased in the colored state and increased in the bleached state where TNTs exhibited better electrochromic properties than a-TNTs. A factor of this crystal structure is well known in that it makes ion penetration in the films more difficult, namely a decrease in the electrochromic properties. The formation of nanostructured films to increase the surface area is therefore very necessary to solve the problem of crystal structure [26,35]. In this work, TNTs structure was shown for amorphous structure (TNTs) giving better electrochromic properties than crystal

structure (a-TNTs). This result showed good concordance with the research of Au *et al.* [25]. Moreover, the change in the morphology of TNTs, together with their larger diameter and bamboo-like structure, showed higher electrochromic properties. The transmittance variation ( $\Delta T$ ) is defined in Equation (3). The results showed the highest  $\Delta T$  value at the TNTs3 condition of 12.58% compared to TNTs2 and TNTs1 with values of 4.00% and 1.93%, respectively.

$$\Delta T = T_{\text{bleached}} - T_{\text{colored}} \quad (3)$$

where  $T_{\text{bleached}}$  and  $T_{\text{colored}}$  represent the transmission at the wavelength of 550 nm of bleached and colored states, respectively.

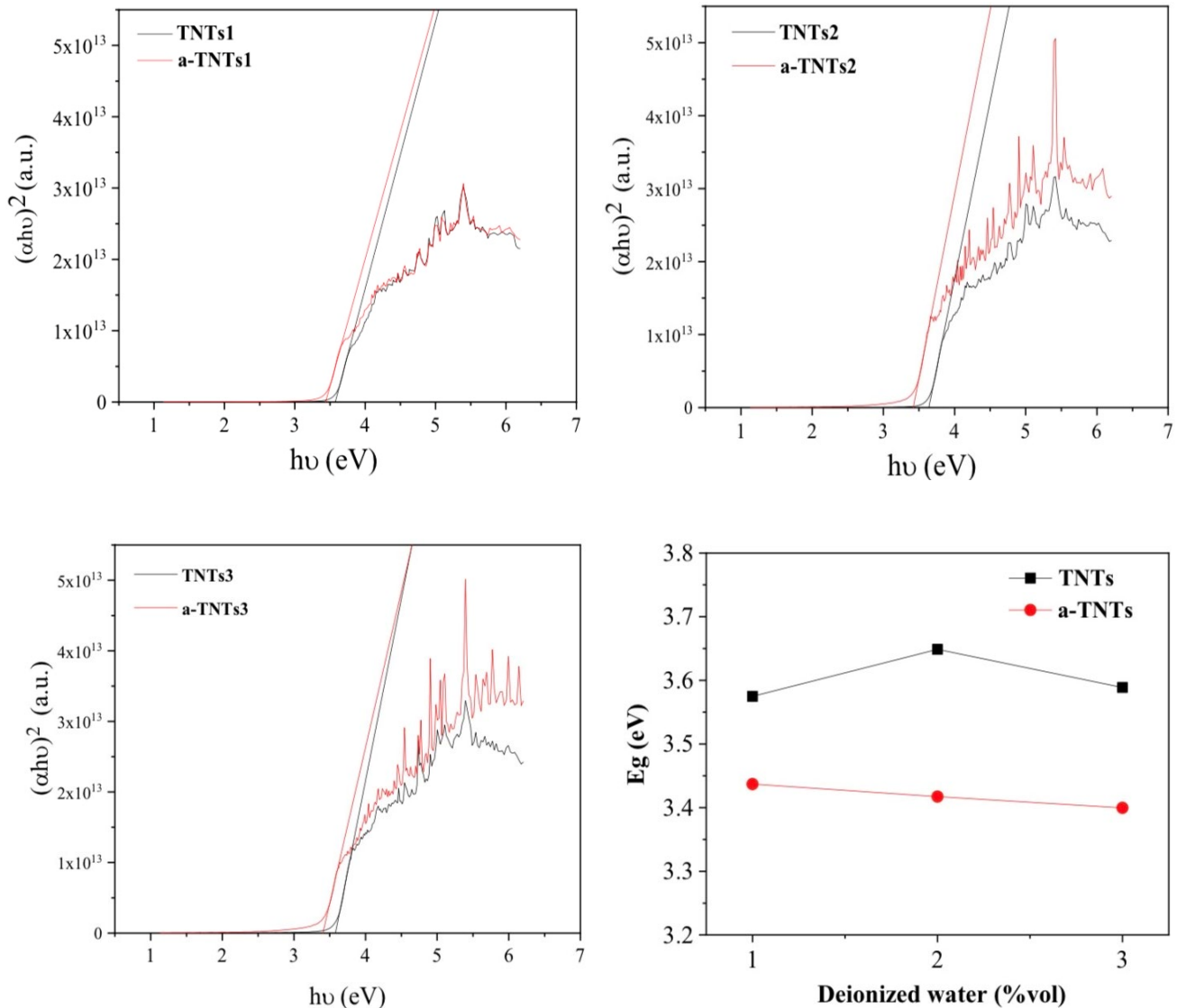


Figure 5. Tauc plot for band gap determination of TNTs before and after annealing.

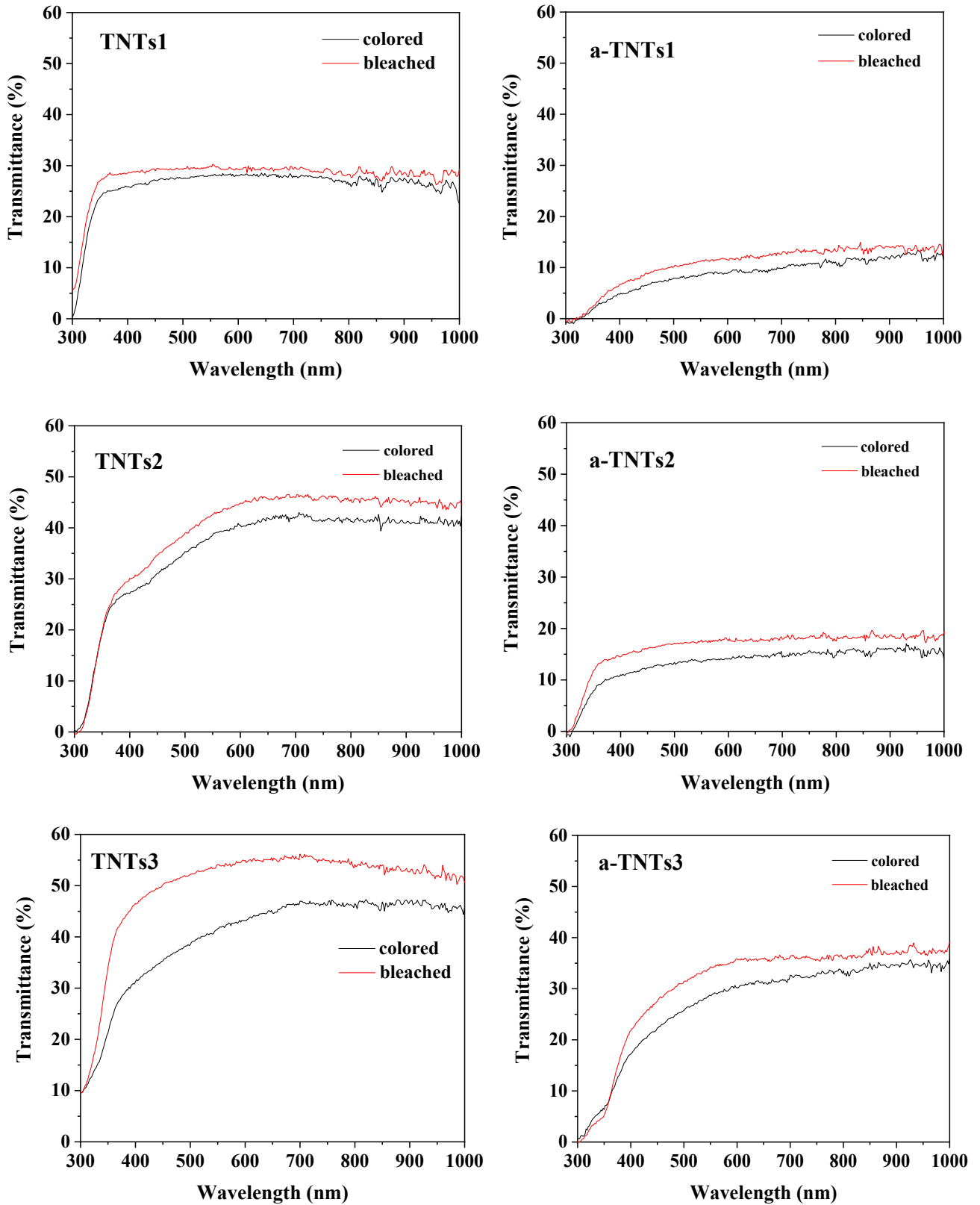


Figure 6. UV-Vis transmittance spectra of TNTs and a-TNTs for colored and bleached states.

#### 4. Conclusions

The TNTs structure was synthesized by an anodizing process from sputtered Ti film by adjusting the deionized water content to change the morphology as well as tube length and diameter. Increasing the deionized water content resulted in larger tube diameters and deionized water of 2 vol% also maximized the length of the TNTs structure. Moreover, the structure of TNTs exhibited similar to bamboo structure with clear separation of each tube for deionized water of 3 vol%. The TNTs film annealing resulted in an anatase phase crystal structure arrangement where the increased deionized water content allowed for a larger crystalline size. In addition, annealed TNTs also reduced the Eg and tended to decrease with increasing deionized water content. In the electrochromic properties test, the bamboo-like structure exhibited the best properties in the non-annealed condition with the highest  $\Delta T$  value of 12.58%.

#### Acknowledgements

The authors gratefully acknowledge the financial support from the Thammasat University research fund, contact No TUFT 36/2566, Thailand. The authors would like to thank the Department of Physics, Faculty of Science and Technology for providing the experimental facilities.

#### References

- [1] Z. Zhang, H. Liu, L. Zhai, J. Wu and L., Li, "Construction of BiOCl-TNTs photoelectrochemical sensor for detection of hydrogen peroxide," *Chemical Physics Letters*, vol. 811, pp. 140177, 2023.
- [2] J. Sivapatarnkun, and K. S. Pudwat, "Effects of active area on UV detection by TiO<sub>2</sub>-sputtered films," *Materials Today: Proceedings*, vol. 47, pp. 3487-3491, 2021.
- [3] S. Niu, W. Yang, H. Wei, M. Danilov, I. Rusetskiy, K.C. Popat, Y. Wang, M. J. Kipper, L. A. Belfiore, and J. Tang, "Heterostructures of cut carbon nanotube-filled array of TiO<sub>2</sub> nanotubes for new module of photovoltaic devices," *Nanomaterials*, vol. 12, pp. 3604, 2022.
- [4] X. Qiu, Z. Wan, M. Pu, X. Xu, Y. Ye, and C. Hu, "Synthesis and photocatalytic activity of Pt-deposited TiO<sub>2</sub> nanotubes (TNT) for Rhodamine B degradation," *Frontiers in Chemistry*, vol.10, p. 922701, 2022.
- [5] C. Salawan, A. Muakngam, B. Sukbot, K. Aiempnanakit, and S. Dumrongrattana, "Effect of DC power on structural and hydrophilic activity of TiO<sub>2</sub> films," *Advanced Materials Research*, vol. 55-57, pp. 925-928, 2008.
- [6] J. Xiong, A. Fei, L. Yu, L. Xia, C. Xu, S. Chen, G. Jiang, and S. Yuan, "Crystal phase-dependent electrochromic performance of porous titanium dioxide nanotube films," *International Journal of Electrochemical Science*, vol. 16, pp.1-12, 2021.
- [7] D. D. Yao, M. R. Field, A. P. O'Mullane, K. K.-zadeh, and J. Z. Ou, "Electrochromic properties of TiO<sub>2</sub> nanotubes coated with electrodeposited MoO<sub>3</sub>," *Nanoscale*, vol. 5, pp. 10353-10359, 2013.
- [8] C. Aiempnanakit, and K. Aiempnanakit, "Structural development and phase transformation behavior of thermally-oxidization Ti by sputtering power and OAD technique," *Materials Chemistry and Physics*, vol. 280, p. 125814, 2022.
- [9] J. Song, R. Guan, M. Xie, P. Dong, X. Yang, and J. Zhang, "Advances in electrospun TiO<sub>2</sub> nanofibers: Design, construction, and applications," *Chemical Engineering Journal*, vol. 431, p. 134343, 2022.
- [10] C. Eyovge, C. S. Deenen, F. R.-Zepeda, S. Bartling, Y. Smirnov, M. M.-Masis, A. S.-Arce, and H. Gardeniers, "Color tuning of electrochromic tio<sub>2</sub> nanofibrous layers loaded with metal and metal oxide nanoparticles for smart colored windows," *ACS Applied Nano Materials*, vol.4, no. 8, pp. 8600-8610, 2021.
- [11] B. Dai, C. Wu, and Y. Xie, "Boosting the electrochromic performance of TiO<sub>2</sub> nanowire film via successively evolving surface structure," *Science China Chemistry*, vol. 64, no. 5, pp. 745-752, 2021.
- [12] P. Junbang, C. Aiempnanakit, and K. Aiempnanakit, "Effects of sputtering power of Ti films on morphology of TiO<sub>2</sub> nanotubes synthesized via anodization process," *Journal of Metals, Materials and Minerals*, vol. 32, no. 2, pp. 24-33, 2022.
- [13] D. Regonini, A. Jaroenworuluck, R. Stevens, and C. R. Bowen, "Effect of heat treatment on the properties and structure of TiO<sub>2</sub> nanotubes: phase composition and chemical composition," *Surface and Interface Analysis*, vol. 42, no. 3, pp.139-144, 2010.
- [14] A. Z. Sadek, H. Zheng, K. Latham, W. Wlodarski, and K. K.-zadeh, "Anodization of Ti thin film deposited on ITO," *Langmuir*, vol. 25, pp. 509-514, 2009.
- [15] M. Szkoda, A. Lisowska, K. Grochowska, L. Skowronski, J. Karczewski, and K. Siuzdak, "Semi – transparent ordered TiO<sub>2</sub> nanostructures prepared by anodization of titanium thin films deposited onto the FTO substrate," *Applied Surface Science*, vol. 381, pp. 36-41, 2016.
- [16] V. S. Simi, and N. Rajendran, "Influence of tunable diameter on the electrochemical behavior and antibacterial activity of titania nanotubes arrays for biomedical applications," *Materials Characterization*, vol. 129, pp. 67-79, 2017.
- [17] P. Yang, Y. Liu, S. Chen, J. Ma, J. Gong, T. Zhang, and X. Zhu, "Influence of H<sub>2</sub>O<sub>2</sub> and H<sub>2</sub>O content on anodizing current and morphology evolution of anodic TiO<sub>2</sub> nanotubes," *Materials Research Bulletin*, vol. 83, pp. 581-589, 2016.
- [18] S. P. Albu, D. Kim, and P. Schmuki, "Growth of aligned TiO<sub>2</sub> bamboo-type nanotubes and highly ordered nanolace," *Angewandte Chemie International Edition*, vol. 47, pp. 1916-1919, 2008.
- [19] V. Sivaprakash, and R. Narayana, "Synthesis of TiO<sub>2</sub> nanotubes via electrochemical anodization with different water content," *Materials today: proceeding*, vol. 37, no. 2, pp. 142-146, 2021.
- [20] D. Kim, A. Ghicov, S. P. Albu, and P. Schmuki, "Bamboo-type TiO<sub>2</sub> nanotubes: Improved conversion efficiency in dye-sensitized solar cells," *Journal of the American Chemical Society*, vol. 130, no. 49, pp. 16454-16455, 2008.
- [21] K. Siuzdak, M. Szkoda, M. Sawczak, J. Karczewski, J. Ryl, and A. Cenian, "Ordered titania nanotubes layer selectively annealed by laser beam for high contrast electrochromic switching," *Thin Solid Films*, vol. 659, pp. 48-56, 2018.

- [22] A. Ghicov, H. Tsuchiya, R. Hahn, J. M. Macak, A. G. Muñoz, and P. Schmuki, "TiO<sub>2</sub> nanotubes: H<sup>+</sup> insertion and strong electrochromic effects," *Electrochemistry Communications*, vol. 8, no. 4, pp. 528-532, 2006.
- [23] M. Molaci, A. F.-alhosseini, M. Nouri, P. Mahmoodi, and A. Nourian, "Incorporating TiO<sub>2</sub> nanoparticles to enhance corrosion resistance, cytocompatibility, and antibacterial properties of PEO ceramic coatings on titanium," *Ceramics International*, vol. 48, no. 14, pp. 21005-21024, 2022.
- [24] C. Salawan, M. Aiempnanakit, K. Aiempnanakit, C. Chananonawathom, P. Eiamchai, and M. Horprathum, "Effects of oblique angle deposition on optical and morphological properties of WO<sub>3</sub> nanorod films for electrochromic application," *Materials Today: Proceedings*, vol. 4, pp. 6423-6429, 2017.
- [25] B. W.-C. Au, A. Tamang, D. Knipp, and K.-Y. Chan, "Post-annealing effect on the electrochromic properties of WO<sub>3</sub> films," *Optical Materials*, vol. 108, p. 110426, 2020.
- [26] C. Aiempnanakit, R. Momkhunthod and K. Aiempnanakit, "Electrochromism in nanoporous tungsten trioxide films prepared through anodization and thermal oxidation," *Integrated Ferroelectrics*, vol. 222, pp. 84-92, 2022.
- [27] C. Aiempnanakit, A. Chanachai, N. Kanchai, M. Aiempnanakit and K. Aiempnanakit, "Electrochromic property of tungsten trioxide films prepared by DC magnetron sputtering with oblique angle deposition and thermal oxidation," *Journal of Metals, Materials and Minerals*, vol. 31, no. 2, pp. 123-128, 2021.
- [28] W. Thongjoon, I. Chuasontia, K. Aiempnanakit, and C. Aiempnanakit, "Morphology and electrochromic property of chemical bath deposited NiO films at different NiSO<sub>4</sub> concentration," *Journal of Metals, Materials and Minerals*, vol. 32, no. 4, pp. 87-92, 2022.
- [29] S. Q. Jin, S. S. Wen, M. Y. Li, H. Zhong, Y. W. Chen, and H. G. Wang, "Effect of the grain size on the electrochromic properties of NiO films," *Optical Materials*, vol. 109, pp. 110280-110288, 2020.
- [30] J. R. Abenez Acuña, I. Perez, V. Sosa, F. Gamboa, J. T. Elizalde, R. Fariás, D. Carrillo, J. L. Enríquez, A. Burrola, and P. Mani, "Sputtering power effects on the electrochromic properties of NiO films," *Optik - International Journal for Light and Electron Optics*, vol. 231, pp. 166509-166524, 2021.
- [31] P. Li, S. Dai, D. Dai, Z. Zou, R. Wang, P. Zhu, K. Liang, F. Ge, and F. Huang, "Influence of the microstructure of sputtered Ti films on the anodization toward TiO<sub>2</sub> nanotube arrays," *Chemical Physics Letters*, vol. 826, p. 140675, 2023.
- [32] D.-J. Won, C.-H. Wang, H.-K. Jang, and D.-J. Choi, "Effects of thermally induced anatase-to-rutile phase transition in MOCVD-grown TiO<sub>2</sub> films on structural and optical properties," *Applied Physics A*, vol. 73, pp. 595-600, 2001.
- [33] K. M. Reddy, S. V. Manorama, and A. R. Reddy, "Bandgap studies on anatase titanium dioxide nanoparticles," *Materials Chemistry and Physics*, vol. 3, pp. 239-245, 2003.
- [34] Z. Tong, J. Hao, K. Zhang, J. Zhao, B.-L. Suc, and Y. Li, "Improved electrochromic performance and lithium diffusion coefficient in three-dimensionally ordered macroporous V<sub>2</sub>O<sub>5</sub> films," *Journal of Materials Chemistry C*, vol. 2, pp. 3651-3658, 2014.
- [35] J. Z. Ou, S. Balendhran, M. R. Field, D. G. McCulloch, A. S. Zoolfakar, R. A. Rani, S. Zhuykov, A. P. O'Mullane, and K. Kalantar-zadeh, "The anodized crystalline WO<sub>3</sub> nanoporous network with enhanced electrochromic properties," *Nanoscale*, vol. 4, no. 19, pp. 5980-5988, 2012.